Provided for non-commercial research and education use.
Not for reproduction, distribution or commercial use.

Volume 71, April 2014

ISSN 0017-9310

ELSEVIER

International Journal of
HEAT and MASS
TRANSFER

Editor-in-Chief
W. J. MINKOWYCZ

Editors
A. R. BALAKRISHNAN, P. CHENG, R. GREIF, C. P. GRIGOROPOULOS,
B. WEIGAND, A. I. LEONTIEV, J. W. ROSE, J. TAINE, H. YOSHIDA

Available online at www.sciencedirect.com

ScienceDirect

This article appeared in a journal published by Elsevier. The attached copy is furnished to the author for internal non-commercial research and education use, including for instruction at the authors institution and sharing with colleagues.

Other uses, including reproduction and distribution, or selling or licensing copies, or posting to personal, institutional or third party websites are prohibited.

In most cases authors are permitted to post their version of the article (e.g. in Word or Tex form) to their personal website or institutional repository. Authors requiring further information regarding Elsevier's archiving and manuscript policies are encouraged to visit:

http://www.elsevier.com/authorsrights

International Journal of Heat and Mass Transfer 71 (2014) 515–520

Contents lists available at ScienceDirect

International Journal of Heat and Mass Transfer

journal homepage: www.elsevier.com/locate/ijhmt

Optimization of near-infrared laser drilling of silicon carbide under water

Naoki Iwatani, Hong Duc Doan *, Kazuyoshi Fushinobu

Tokyo Institute of Technology, Box I6-3 Meguro-ku, Tokyo 152-8550, Japan

ARTICLE INFO

Article history:
Received 16 January 2013
Received in revised form 28 October 2013
Accepted 14 December 2013
Available online 14 January 2014

Keywords:
Liquid-assisted laser processing
Silicon carbide
Crack
Debris
Heat affect zone
Surface quality

ABSTRACT

Laser drilling of silicon carbide (SiC) wafer in air (dry ablation) and underwater by using ns pulsed infrared (1064 nm) Nd:YAG laser is investigated. In order to suggest optimal parameters of via processing in SiC wafer, the effects of pulse number, laser fluence, water film thickness, and focus position are evaluated. As compared with dry ablation vias, decreasing etching rate, increasing via diameter, and generation of cracks in high-energy regime are observed in liquid-assisted processing. However, it is found that it can create vias without debris, HAZ, cracks. Also, optimal parameter set for infrared pulse laser processing under water is found to be the laser fluence of less than 10 J/cm^2 and water thickness of 1 mm.

© 2013 Elsevier Ltd. All rights reserved.

1. Introduction

The success of microelectronics has been followed by rapid development in microelectro-mechanical systems (MEMS) where silicon (Si) is currently the leading material. Nowadays there is an increased demand for devices capable of functioning at high temperatures and in harsh environments, which exceed the physical properties of Si. This demand accounts for the emergence of SiC, with higher band-gap, higher breakdown threshold, higher thermal conductivity and higher saturation velocity than Si, as preferred material for MEMS in the future.

Unfortunately some of the properties of SiC are also barriers to the fabrication of microelectronics and MEMS devices. Conventional dry etching techniques of via through SiC wafers requires time-consuming mechanical thinning to a thickness of $\sim$100 μm. Typical etch rates for 4H and 6H SiC substrates in F$_2$- or Cl$_2$-based plasmas range between 0.2 μm/min and 1.3 μm/min [1–4]. In contrast to the chemical-based micro-fabrication methods, laser ablation of SiC is capable of higher etching rates [5–7] and precise control of via size with advancement of the reduction in the number of processing steps as masking, machining independent of crystal structure, and curved surfaces. Laser ablation of SiC has been carried out with pulse durations from nanosecond to femtosecond regime. Femtosecond lasers have produced little contamination and low HAZ (heat affected zone) [8–10]. However, the lower etch rates via formation compared with nanosecond laser and the high cost of machining system still is the problem to spread out. In the practical system, the ns pulse laser machining is widely used.

Single-crystalline SiC is practically transparent at visible wavelengths, but has an optical absorption on the order of 10^5 cm^{-1} in the UV regime due to the intrinsic absorption of photon energy. Nanosecond pulsed UV lasers such as excimer and frequency tripled and quadrupled Nd:YAG are the most widely used [11–14] due to their prevalence and the high optical absorption of crystalline SiC at UV wavelengths. It is concluded that UV laser ablation is an effective but slow material removal process for SiC wafers compared to infrared lasers such as 1064 nm Nd:YAG [14]. However, it is well known that near-infrared laser micromachining can be quite complicated by collateral thermal effect such as melt, recast and HAZ.

Recently, there have been increasing studies on liquid-assisted laser micromachining, in particular, laser drilling of a work piece under water. It has been reported that liquid-assisted laser micromachining can reduce the extent of HAZ, micro-cracks, sputter redeposition and tapering of drilling [11–13]. The etching rate on liquid-assisted laser drilling strongly depends on liquid film thickness [14–15]. The reduction of the extent of HAZ, micro-cracks, and sputter redeposition can be explained by the cooling effect of the liquid. However, the dependence of etching rate on liquid film thickness and the detailed processing parameters are still unclear because of the change of laser profile and energy during its propagation in water film [16]. That is one of issues for spread out

---

* Corresponding author. Tel./fax: +81 03 5734 2500.
E-mail address: doan.d.aa@m.titech.ac.jp (H.D. Doan).

0017-9310/$ - see front matter © 2013 Elsevier Ltd. All rights reserved.
http://dx.doi.org/10.1016/j.ijheatmasstransfer.2013.12.046

liquid-assisted laser micromachining technique. The authors have investigated the laser propagation in various media both experimentally and numerically [16–18]. In this study, the detailed processing parameters in liquid-assisted laser micromachining will also be discussed based on the propagation characteristics of the laser beam during its propagation under water.

In this study, the efficiency and quality of pulsed-laser drilling of SiC in the air and under water are investigated and compared. Besides in order to suggest optimal parameters of via processing in SiC wafer, the effects of pulse number, laser fluence, water film thickness, and focus position are evaluated.

2. Experimental set-up

2.1. Experimental set-up and methodology

Fig. 1 represents the experimental set-up geometry. Laser beam has been set to focus on the surface of SiC wafer in the air. The SiC wafer was immersed in water film with a thickness of 0.5 mm, 1.0 mm, and 1.5 mm during laser drilling. The thickness of water film is deposited by diving the injected water volume (measured value) by the area of the cuvette (31.5 mm × 31.5 mm). A commercial 4H–SiC wafer (10 mm × 10 mm × 0.34 mm) was used for laser drilling. The SiC sample is doped with nitrogen. The concentration of nitrogen was measured by using secondary ion mass spectrometry method as the depth-wise profile of concentration with concentration of $1.8 \times 10^{20}\ \mathrm{cm}^{-3}$ at the surface and $1.6 \times 10^{19}\ \mathrm{cm}^{-3}$ in the bulk.

The near-infrared nanosecond laser used in this work was an Nd: YAG laser (Continuum Surelite I-10, $P = 4.72$ W, $\lambda = 1064$ nm) with the pulse duration of 6 ns. The laser is operated in the TEM_{00} mode, and the laser beam profile is Gaussian, which was measured by a CCD camera. The pulse energy was controlled by an external attenuator including a variable beam splitter and a correction plate. After focused by a 10× object lens, pulse energies were measured by using an energy meter. The quality of processing was evaluated with an optical microscope (KEYENCE VF7500) and a scanning electron microscope (KEYENCE VE8800). The detailed experimental parameters are shown in Table 1.

2.2. Relationship between water film thickness and focal position

When a workpiece is immersed in the water film, it is required to reset the focus on the workpiece surface according to conditions. In order to compare the focal position in the air and that under water, the difference was measured. The displacement from the focal position in the air is defined as "defocus". The defocus opposite to the sample surface is defined as positive value. Fig. 2 shows the

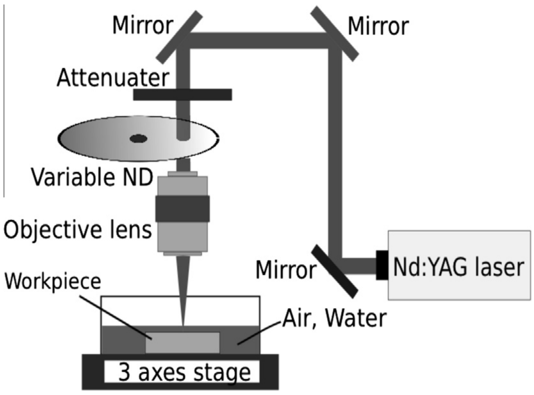

Fig. 1. Schematic of the experimental set up.

Table 1
Experimental parameter.

Parameter	Value
Wavelength	1064 nm
Repetition rate	10 Hz
Pulse width	5–7 ns
Objective lens	10×
Beam spot size	29.4 μm
Focus position	Surface

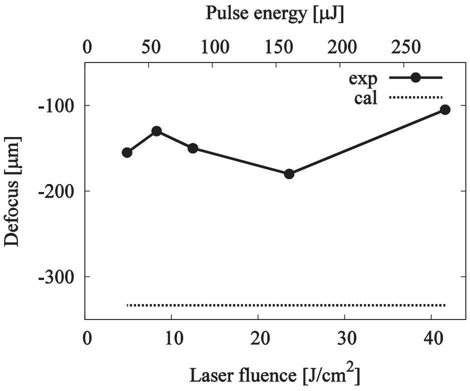

Fig. 2. Plot of squared diameter against energy per pulse. Vertical and horizontal axes show depth from defocus and laser fluence (pulse energy), respectively.

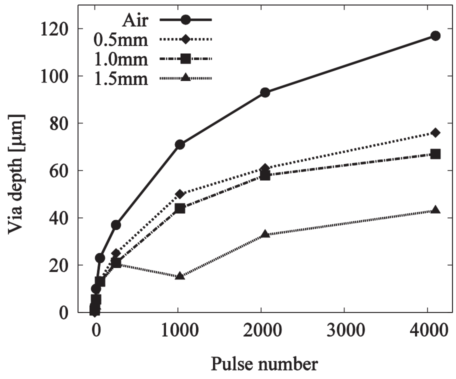

Fig. 3. Relationship between via depth and pulse number. Vertical and horizontal axes show etching rate and thickness of water film, respectively.

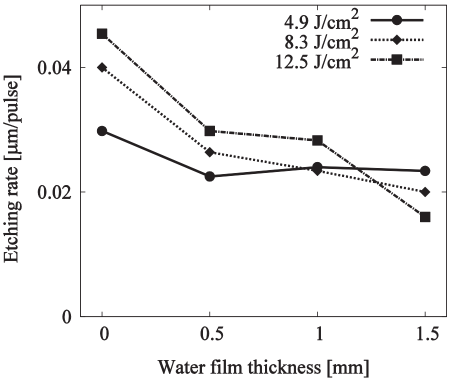

Fig. 4. Relationship between etching rate and thickness of water film. Vertical and horizontal axes show etching rate and thickness of water film, respectively. Here, the etching rate is measure after 2048 pulses of laser irradiation.

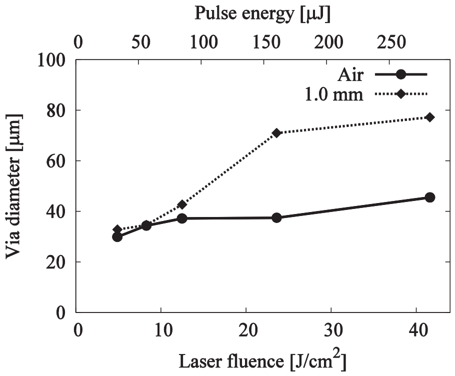

Fig. 5. Relationship between via diameter and laser fluence for the processing in air and water. Vertical and horizontal axes show via diameter and laser fluence (pulse energy), respectively.

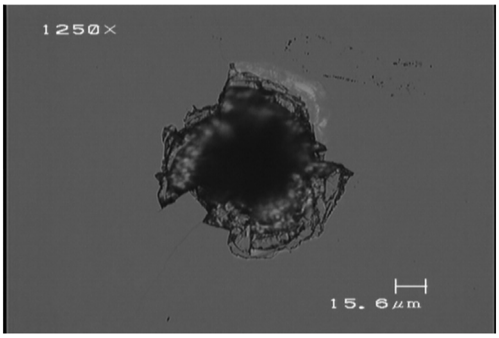

Fig. 6. Laser microscope image of cracks.

Pulse number

Lase fluence [J/cm²]	1	4	16	64	256	1024	2048	4096
189.4					▨	▨	▨	▨
87.1		▨			▨	▨	▨	▨
41.6							▨	
23.6								▨
12.5								
8.3								

※ ▨ : crack

Fig. 7. Relationship between the generation of cracks and the condition of pulse number and laser fluence.

defocus as a function of laser fluence for 1.0 mm thickness water film. The dotted line shows a theoretical estimate based on Snell law to a laser beam incident on the interface between air and water. As a result, it is found that the focal position under water is located between that in the air and the estimated position. With the increasing of laser fluence, defocus is fluctuated. When laser pulse is focused in the water film the focal point will be moved out of the set-up focal point in air cause by 2 reasons. First, the focal length is longer in water because the incidence or refraction of water (1.33) is higher than that of air (almost 1.0). The increase of focal length is proportional to the water film thickness. The other is the due to the nonlinear optical effects including optical Kerr effect and plasma defocusing. When the laser intensity becomes very high, change of water refractive index depends to the intensity of the laser. This causes self-focusing and shorter focal length. As the result, the peak laser fluence at wafer surface is higher than that of focusing in the air. As the intensity of the self-focused spot increases beyond a certain value, the water is ionized by the high local laser field. This lowers the refractive index, resulting in defocus of the propagating light beam. The change of focal position for the laser fluence occurs because of changing the balance of self-focusing and defocusing. Therefore, it is required to reset a focal position when the water film thickness and pulse energy are changed.

3. Results and discussions

3.1. Effects of pulse number and water film thickness on etching rate

Fig. 3 shows the relationship between via depth and pulse number. Vertical and horizontal axes show etching rate and water film thickness, respectively. The via depth increases non-linearly with increasing the pulse number and tends to be saturated. Rayleigh length is calculated as approximately 240 μm in this optical system. Since the laser beam was focused on the SiC surface, the suitable region for laser drilling is estimated approximately 120 μm as a half of Rayleigh length. The depth is therefore tends to be saturated at around this value.

Fig. 4 shows the relationship between etching rate and thickness of water film. Vertical and horizontal axes show etching rate and thickness of water film, respectively. Here, the etching rate is measure after 2048 pulses of laser irradiation. In the case of liquid-assisted processing, the etching rate becomes lower. It decreases with increasing water film thickness, as shown in Fig. 4. From these results, it is suggested that the energy is absorbed by the ionization of water and the energy reaching the workpiece becomes smaller as discussed in previous work [16]. However, the influence of the liquid film thickness is very small for the lowest energy (=4.9 J/cm^2.) This can be due to the decreasing water ionization resulting from the decreasing pulse energy. Thin water film is therefore better from the viewpoint of energy

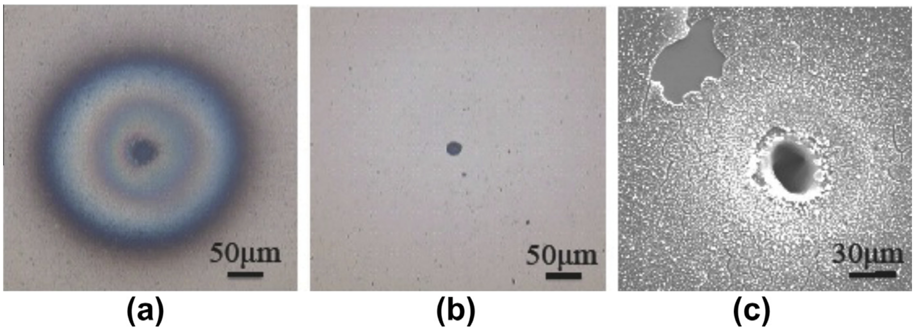

Fig. 8. SEM image of SiC surface after ablated in air and under water.

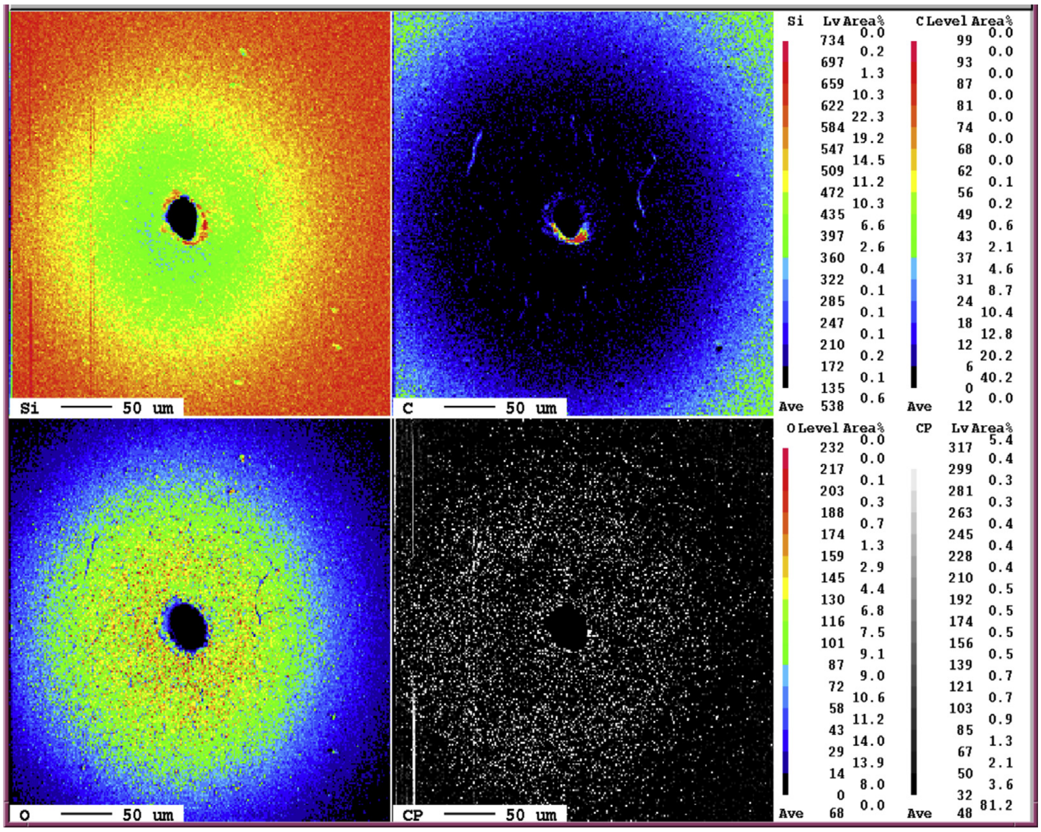
Si 50 um
C 50 um
O 50 um
CP 50 um
Si Lv Area%
734 697 659 622 584 547 509 472 435 397 360 322 285 247 210 172 135 Ave 538
0.0 0.2 1.3 10.3 22.3 19.2 14.5 11.2 10.3 6.6 2.6 0.4 0.1 0.1 0.1 0.2 0.1 0.6
C Level Area%
99 93 87 81 74 68 62 56 49 43 37 31 24 18 12 6 0 Ave 12
0.0 0.0 0.0 0.0 0.0 0.0 0.0 0.1 0.2 0.6 2.1 4.6 8.7 10.4 12.8 20.2 40.2 0.0
O Level Area%
232 217 203 188 174 159 145 130 116 101 87 72 58 43 29 14 0 Ave 68
0.0 0.0 0.1 0.3 0.7 1.3 2.9 4.4 6.8 7.5 9.1 9.0 10.6 11.2 14.0 13.9 8.0 0.0
CP Lv Area%
317 299 281 263 245 228 210 192 174 156 139 121 103 85 67 50 32 Ave 48
5.4 0.4 0.3 0.3 0.4 0.4 0.4 0.5 0.5 0.5 0.5 0.7 0.7 0.9 1.3 2.1 3.6 81.2

(a) in air

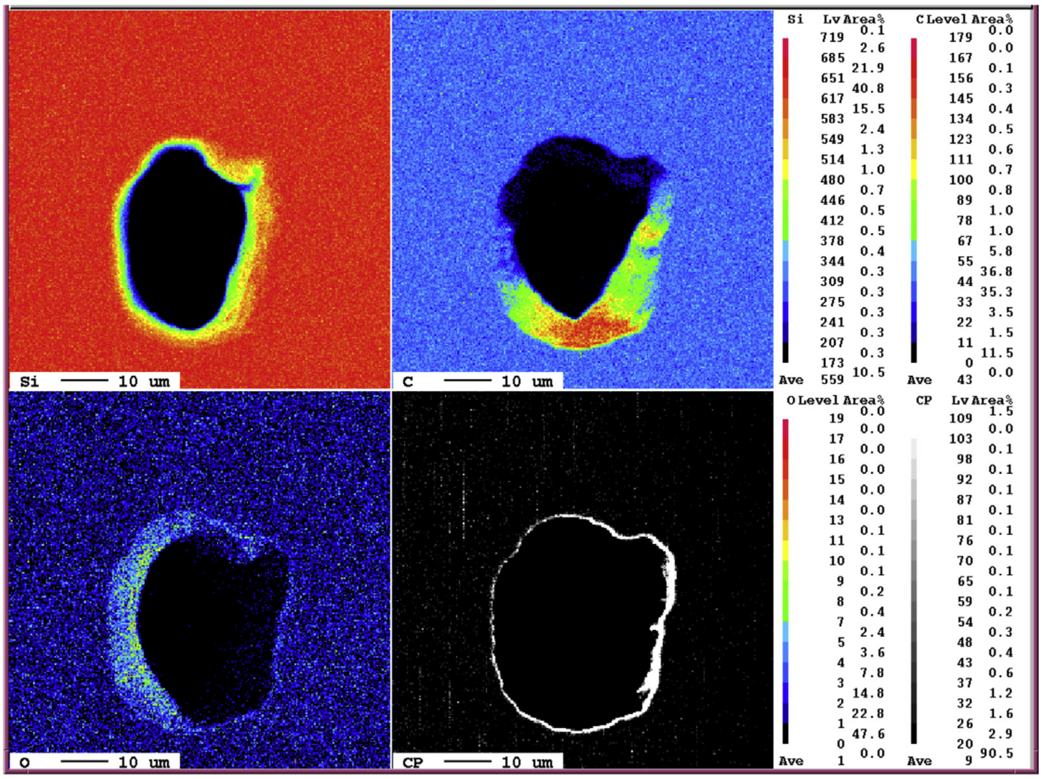
Si 10 um
C 10 um
O 10 um
CP 10 um
Si Lv Area%
719 685 651 617 583 549 514 480 446 412 378 344 309 275 241 207 173 Ave 559
0.1 2.6 21.9 40.8 15.5 2.4 1.3 1.0 0.7 0.5 0.5 0.4 0.3 0.3 0.3 0.3 0.3 10.5
C Level Area%
179 167 156 145 134 123 111 100 89 78 67 55 44 33 22 11 0 Ave 43
0.0 0.0 0.1 0.3 0.4 0.5 0.6 0.7 0.8 1.0 1.0 5.8 36.8 35.3 3.5 1.5 11.5 0.0
O Level Area%
19 17 16 15 14 13 11 10 9 8 7 5 4 3 2 1 0 Ave 1
0.0 0.0 0.0 0.0 0.0 0.0 0.1 0.1 0.1 0.2 0.4 2.4 3.6 7.8 14.8 22.8 47.6 0.0
CP Lv Area%
109 103 98 92 87 81 76 70 65 59 54 48 43 37 32 26 20 Ave 9
1.5 0.0 0.1 0.1 0.1 0.1 0.1 0.1 0.1 0.1 0.2 0.3 0.4 0.6 1.2 1.6 2.9 90.5

(b) Under water

Fig. 9. EPMA analysis of the via surface processed.

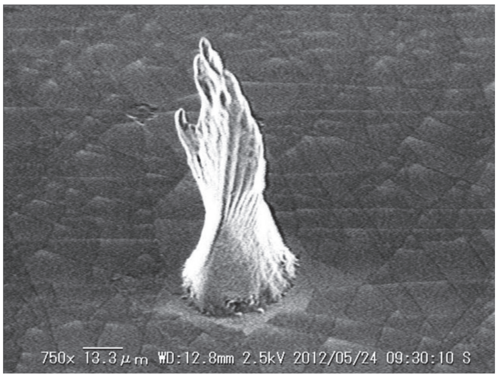

(a) Air, fluence: 8.3 J/cm^2, number of pulses: 2048

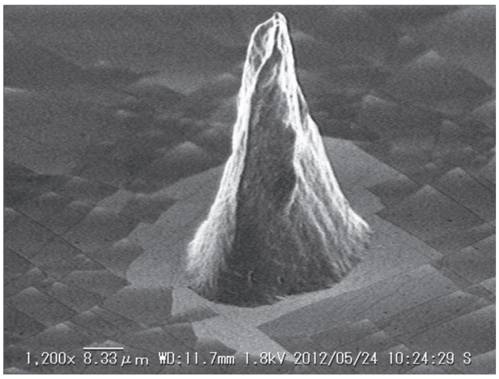

(b)Water thickness: 1.0 mm, fluence: 23.6 J/cm^2, number of pulses: 2048

Fig. 10. SEM images of the hole mold drilled in air and under water respectively.

efficiency. From the viewpoint of process condition setting, it is difficult to maintain the 0.5 mm water film because the surface tension and the impact during processing easily break the film structure. Considering in conjunction with energy efficiency, a suitable liquid film thickness is proposed to be around 1.0 mm.

This method has unstable conditions where the etching rate drops sharply (Fig. 3: 1.5 mm, $n = 1024$). Since many factors influence the process quality, such as nonlinear optical effect, ionization of water, generation of bubbles, and particles emission, it is necessary to fine-tune the control process conditions.

3.2. Effects of laser fluence and pulse number on crack generation

Fig. 5 shows the relationship between via diameter and laser fluence for the processing in air and water. Vertical and horizontal axes show via diameter and laser fluence (pulse energy), respectively. When the laser fluence is greater than about 10 J/cm^2, via diameter tends to increase rapidly, as shown in Fig. 5. Fig. 6 shows laser microscope image of cracks. These results show that the generation of cracks spread via diameter at higher laser fluence. In other words, the vias can be formed to be smaller than or equal to those processed in the air if the cracks do not appear.

Fig. 7 shows the relationship between the generation of cracks and the condition of pulse number and laser fluence. When pulse number reaches a certain value for each fluences, cracks appear suddenly. From this result, the mechanism for crack generation can be inferred as follows; In the case of liquid-assisted processing, generation of high pressure by the plasma confinement in the water has been reported [19]. The pressure and thermal stress are applied to SiC during processing. That is repeated by the pulse number, and fatigue is accumulated in SiC. When accumulation of the fatigue reaches a limit, cracks will be generated. Once cracks are generated, the via edge collapses gradually. Therefore, it is important to suppress generation of cracks. From this result, the laser fluence should not exceed about 10 J/cm^2.

On the other hand, the depth shows steady increase with the increasing number of pulses. Despite the slower processing speed, however, it is preferred to create a deep hole by increasing the pulse number rather than increasing the laser fluence.

3.3. Surface quality

Fig. 8(a) and (b) show the laser microscope images of via surface in air and under water, respectively. Discoloration pattern is observed in the case of processing in the air, as shown in Fig. 8(a). This discoloration is observed when the white light is reflected from the top and bottom boundaries of the oxide film on the sample surface. During the drilling process, the samples were superficially melted by the laser beam leading to oxygen diffusion through the molten material and, thus, to the oxidation of SiC. Therefore, the discolored area shows the heat affected zone in surface. The oxidation film consists of SiO_2 (i.e. glass). Its thickness gradually decreases with increasing the distance from the center. Fig. 8(c) shows an SEM image of SiC surface after the EPMA analysis. Fig. 8(a–c) indicates that the oxide film only stays on the flat SiC surfacein the case of dry processing. In the case of liquid-assisted processing, debris and a discoloration area decrease dramatically.

A quantitative analysis by EPMA and an observation by SEM were also carried out. Fig. 9 shows the results of EPMA analysis. Although oxygen was detected from the surface of the via processed in the air, it was not detected from that processed underwater. It was therefore confirmed that the discoloration area is an oxide film. The smaller the distance from the via, the larger the particles on the surface become. From these results, it is suggested that the oxide film was formed by deposition of the debris. Since water carried the discharged particles efficiently and controlled deposition of the debris, oxygen was not detected from the surface of vias processed underwater.

3.4. Influence of beam polarization

To investigate the hole shape, a silicone mold (Ted Pella, Inc.) of the holes was made. Fig. 10(a) and (b) show, respectively, the SEM images of the hole mold drilled in air and under water respectively. The hole, which drilled in air, shows the formation of multiple borehole tails. On the contraty, the hole, which drilled under water, shows the improvement of axially symmetrical geometry. The generation of multiple borehole tails in the hole, which drilled in air, can be explain by change of polarization of laser beam during it multiple reflected in the hole [20–22]. The hole, which drilled under water, have a smaller taper angle and smaller reflectivity. As a consequence, the multiple reflection effect is reduced during drilling processing under water. Therefore, as compared with dry ablation vias, drilling hole under water improves the axially symmetrical geometry of the hole for deep drilling process.

4. Conclusion

Characteristics of via processing on SiC surface by means of ns pulse near-infrared laser is investigated.

When the workpiece is immersed in a water film, a focus moves to the sample surface, and the amount of defocus changes by self-focusing and plasma defocusing. Therefore, it is required to reset a focal position when the water film thickness and pulse energy are changed.

As compared with dry ablation vias, decreasing etching rate, increasing via diameter, and generation of cracks in high-energy regime are observed in liquid-assisted processing. Especially processing with high fluence has several drawbacks, such as change of the focus by ionization of water, generating of cracks However, it is found that it can create vias without debris, HAZ, cracks, and optimal parameter for infrared pulse laser processing under water by fine-tuning the parameters.

Drilling hole under water reduces multiple reflection effect, improves the axially symmetrical geometry of the hole for deep drilling process.

Acknowledgements

Part of this work has been supported by the Grant-in-Aid for Scientific Research by MEXT/JSPS and the Amada Foundation. HDD acknowledges the support from JSPS. We appreciate the help received from Tokyo Institute of Technology Center for Advanced Materials Analysis for SEM and EPMA analysis.

References

[1] P.H. Yih, A.J. Steckl, Residue-free reactive ion etching of silicon carbide in fluorinated plasmas II, J. Electrochem. Soc. 142 (2853) (1995) 312–319.

[2] J.R. Flemish, K. Xie, J.H. Zhao, Smooth etching of single crystal 6H–SiC in an electron cyclotron resonance plasma reactor, Appl. Phys. Lett. 64 (1994) 2315–2317.

[3] H. Cho, P. Leerungnawarat, D.C. Hays, S.J. Pearton, S.N.G. Chu, R.M. Strong, C.M. Zetterling, M. Östling, F. Ren, Ultradeep, low-damage dry etching of SiC, Appl. Phys. Lett. 76 (2000) 739–741.

[4] J.J. Wang, E.S. Lambers, S.J. Pearton, M. Ostling, C.M. Zetterling, J.M. Grow, F. Ren, R.J. Shul, Inductively coupled plasma etching of bulk 6H–SiC and thin-film SiCN in NF3 chemistries, J. Vac. Sci. Technol., A 16 (1998) 2204–2209.

[5] S. Kim, B.S. Bang, F. Ren, J. D'entremond, W. Blumenfeld, T. Cordock, S.J. Pearton, SiC via holes by laser drilling, J. Electron. Mater. 33 (2004) 477–480.

[6] S. Kim, B.S. Bang, F. Ren, J. D'entremond, W. Blumenfeld, T. Cordock, S.J. Pearton, High-rate laser ablation for through-wafer via holes in SiC substrates and GaN/AlN/SiC templates, J. Semicond. Technol. Sci. 4 (2004) 217–221.

[7] S.J. Pearton, C.R. Abernathy, B.P. Gila, F. Ren, J.M. Zavada, Y.D. Park, Enhanced functionality in GaN and SiC devices by using novel processing, Solid-State Electron. 48 (2004) 1965.

[8] Y. Dong, P. Molian, n-situ formed nanoparticles on 3C– SiC film under femtosecond pulsed laser irradiation, Phys. Status Solidi A 202 (2005) 1066–1072.

[9] Y. Dong, C.A. Zorman, P. Molian, Femtosecond pulsed micromachining of single crystalline 3C-SiC structures based on a laser-induced defect-activation process, J. Micromech. Microeng. 13 (2003) 680–685.

[10] B. Pecholt, M. Vendan, Y. Dong, P. Molian, Ultra laser micromachining of 3C–SiC thin films for MEMS device fabrication, Int. J. Adv. Manuf. Technol. 39 (2007) 239–250.

[11] S. Zoppel, M. Farsari, R. Merz, J. Zehetner, G. Stangl, G.A. Reider, C. Fotakis, Laser micro machining of 3C–SiC single crystals, Microelectron. Eng. 83 (2006) 1400–1402.

[12] R.F. Wood, D.H. Lowndes, Laser processing of wide bandgap semiconductors and insulators, Cryst. Lattice Defects Amorphous Mater. 12 (1985) 475–497.

[13] R. Reitano, P. Baeri, N. Marino, Excimer laser induced thermal evaporation and ablation of silicon carbide, Appl. Surf. Sci. 96–98 (1996) 302–308.

[14] Saurabh Gupta, Ben Pecholt, Pal Molian, Excimer laser ablation of single crystal 4H-SiC and 6H-SiC wafers, J. Mater. Sci. 46 (2011) 196–206.

[15] H. Howard, A.J. Conneely, G.M. O'Connor, T.J. Glynn, Investigation of a method for the determination of the focused spot size of industrial laser beams based on the drilling of holes in mylar film, in: Proceedings of Opto Ireland 2002: Optics and Photonics Technologies and Applications, vol. 4876, 2003, pp. 541–552.

[16] H.D. Doan, N. Iwatani, K. Fushinobu, Laser beam profile shaping on liquid-assisted laser drilling of silicon carbide, ISTP-22, in: Proc. ISTP-22, 2011.

[17] H.D. Doan, Y. Akamine, K. Fushinobu, Fluidic laser beam shaper by using thermal lens effect, Int. J. Heat Mass Transfer 55 (2012) 2807–2812.

[18] Y. Akamine, H.D. Doan, K. Fushinobu. Finite-Difference Time Domain analysis of ultrashort pulse laser light propagation under nonlinear coupling, ISTP-23, in: Proc. ISTP-23, 2012.

[19] V.A. Ageev, A.F. Bokhonov, V.V. Zhukovskii, A.A. Yankovskii, Dynamics of processes occurring in laser ablation of metals in a liquid, J. Appl. Spectrosc. 64 (5) (1997) 683–688.

[20] S. Nolte, C. Momma, G. Kamlage, A. Ostendorf, C. Fallnich, F.vonAlvenslebenH. Welling, Polarization effects in ultrashort-pulse laser drilling, Appl. Phys. A 68 (1999) 563–567.

[21] T.V. Kononenko, V. Konov, S. Garnov, S. Klimentov, F. Dausinger, Dynamics of deep short pulse laser drilling: ablative stages and light propagation, Laser Phys. 11 (3) (2001) 343–351.

[22] Sven Döring, Sören Richter, Stefan Nolte, Andreas Tünnermann, In situ imaging of hole shape evolution in ultrashort pulse laser drilling, Opt. Express 18 (19) (2010) 20395–20400.